# Noncoherent Coded Continuous Phase Modulation

Gerald Enzner*, Lutz Lampe, Robert Schober, Johannes Huber

Institute of Communication Systems and Data Processing*
Aachen University of Technology
Muffeter Weg 3, D–52072 Aachen, Germany
Phone: +49 241 88 6960, E-mail: enzner@ind.rwth-aachen.de

Telecommunications Laboratory
University Erlangen–Nürnberg
Cauerstraße 7/NT, D–91058 Erlangen, Germany
Phone: +49 9131 85 28718, E-mail: LLampe@LNT.de

## Abstract

We discuss convolutionally encoded continuous phase modulation (CPM) with noncoherent detection. Specifically, the application of a feedback–free modulator is considered, which is perfectly suited to coded transmission. Demodulation employs a frequency–sampling receiver with reduced representation of the signal space, whereas the decoder makes use of reduced–state noncoherent sequence estimation (NSE). In particular, NSE means the application of recently proposed noncoherent per–survivor Viterbi processing. Recursive calculation of the implicit phase reference symbol is proposed in this paper to keep the NSE complexity low. Receiver front–end and NSE are optimized separately. The resulting performance is demonstrated by simulations.

## 1 Introduction

Continuous phase modulation (CPM) [1] is an attractive technique for digital communications. Due to its constant envelope, full amplifier power can be exploited without any back–off to avoid amplifier nonlinearities. Additionally, the power efficiency of CPM is improved by the inherent trellis code caused by smoothed phase transitions [2, 3]. For the same reason, CPM is highly bandwidth efficient, too. A noncoherent receiver for CPM avoids the need for explicit carrier phase synchronization. Especially in the case of coded modulation, combined decoding and synchronization is rewarding in terms of robustness of the transmission link. So called *noncoherent sequence estimation (NSE)* techniques are very well suited to channels with slowly time–variant phases [4].

In this paper, the optimization of the noncoherent receiver is performed in two stages on the basis of the decomposition approach for CPM [2, 3]. The decomposition of CPM facilitates the independent design and complexity reduction of a receiver front–end (matched filter) and subsequent NSE, respectively. The receiver front–end presented in [5] is applied here, which requires only two or three matched filters and provides sufficient accuracy at the same time.

For noncoherent CPM detection , we apply a novel NSE scheme which has been previously proposed for coded $M$–ary phase–shift keying (MPSK) and differential MPSK (MDPSK) transmission over intersymbol interference (ISI) channels (cf. [6] and references therein). This NSE scheme enables the recursive calculation of the reference symbol required for metric calculation and thus, offers considerable savings in computational complexity for achieving the same/better power efficiency as/than in [7]/[8]. Also the number of states can be chosen in this approach to satisfy any predetermined complexity constraints.

Simulation results verify that the proposed noncoherent coded CPM scheme enables power–efficient transmission with a very fair demodulation and decoding complexity.

## 2 Transmission System

In this section, we introduce the system model for noncoherent CPM transmission. First, decomposition of the CPM system into a natural trellis–encoder and a memoryless modulator (signal table) is briefly reviewed. In particular, we introduce the concept of phase–state mapping, cf. [2], which is perfectly suited for coded modulation and noncoherent detection. The decomposition model enables the construction of the noncoherent receiver with low complexity as described in Section 3.

### 2.1 CPM Signal Representation

The passband CPM signal has the form [1]

$$s_{HF}(\boldsymbol{a},t)=\sqrt{\frac{2E_s}{T}}\cos\left(2\pi f_c t+2\pi h\sum_{i=0}^{\infty}a[i]q(t-iT)\right) \quad (1)$$

where $f_c$ is the carrier frequency, $E_s$ denotes the signal energy per modulation interval $T$, $h=k/p$ is the rational modulation index with relatively prime integers $k$ and $p$. The information sequence $\boldsymbol{a}=\langle a[i]\rangle$, $i\in\mathbb{N}_0$, consists of $M$–ary elements $a[i]\in\{\pm1,\pm3,\ldots,\pm(M-1)\}$, $M$ even. The *phase pulse* $q(t)$ is normalized as usual such that

$$q(t)=\begin{cases}0 & t\le 0\\ 1/2 & t\ge LT\end{cases}\quad . \quad (2)$$

For a compact representation of $s_{HF}(\boldsymbol{a},t)$ as an equivalent complex baseband (ECB) signal it is convenient to use the transformation frequency $f_0=f_c-h\cdot\frac{M-1}{2T}$, cf. [2, 3, 5], which is different from the carrier frequency $f_c$. Furthermore, we introduce the modified data sequence $\boldsymbol{\beta}$ with components

$$\beta[i]\triangleq\frac{a[i]+M-1}{2}\quad\in\{0,1,\ldots,M-1\}\,. \quad (3)$$

Then, the ECB signal $s(\boldsymbol{\beta},t)$ can be interpreted as a sequence of time–limited signal segments $\rho(\boldsymbol{b}[i],t)$:

$$s(\boldsymbol{\beta},t)=\sum_{i=0}^{\infty}\rho(\boldsymbol{b}[i],t-iT) \quad (4)$$

with $\rho(\boldsymbol{b}[i],t)=0$ for $t\notin[0,T)$ and address vector $\boldsymbol{b}[i]$, which is generated from $\boldsymbol{\beta}$ by a minimum trellis encoder [3, 5]. In particular, using the decomposition approach of CPM [2, 3], a description with $pM^L$ signal elements $\rho(\boldsymbol{b}[i],t)$ addressed by vector

$$\boldsymbol{b}[i]\triangleq[\beta[i],\ldots,\beta[i-L+1],\psi[i-L]] \quad (5)$$

from a trellis with $pM^{L-1}$ states $S[i]\triangleq[\beta[i-1],\ldots,\beta[i-L+1],\psi[i-L]]$ is always possible. The *phase state*

$$\psi[i-L]\triangleq\left(k\cdot\sum_{m=0}^{i-L}\beta[m]\right)\bmod p\,, \quad (6)$$

$\psi[i]\in\{0,1,\ldots,p-1\}$, subsumizes the contributions of all past modulator input data for which the phase pulses have already reached a constant value. The data symbols $(\beta[i],\ldots,\beta[i-L+1])$ determine the phase transient, cf. [5]. Thus, the time limited signal elements are given by

$$\rho(\boldsymbol{b}[i],t)=\sqrt{\frac{E_s}{T}}\cdot\mathrm{e}^{\mathrm{j}\frac{2\pi}{p}\psi[i-L]}\cdot\mathrm{e}^{\mathrm{j}4\pi h\sum_{m=0}^{L-1}\beta[i-m]q(t+mT)}\cdot\mathrm{e}^{\mathrm{j}\sum_{m=0}^{L-1}\varphi(t+mT)}\quad\text{for } t\in[0,T) \quad (7)$$

and $\rho(\boldsymbol{b}[i],t)=0$, otherwise, where $\varphi(t)\triangleq 2\pi h(M-1)\left(\frac{t}{2LT}-q(t)\right)$, $0\le t<LT$, accounts for the modified data symbols $\beta[i]$ and the transformation frequency $f_0$ [2, 3, 5].

This model of the CPM modulator with the inherent trellis encoder is refered to as CPM with *frequency mapping*. The contained recursive structure due to (6) is analogous to the well–known differential encoder of DPSK and essentially resolves phase ambiguities.

### 2.2 Phase–State Mapping and Coding

In the above description of CPM, data symbols are mapped to phase changes. However, a mapping to the absolute phase is also possible, cf. [2, 3]. For the interesting special case $M=p$ the unique relation

$$(k\cdot\beta[i])\bmod p=(\psi[i]-\psi[i-1])\bmod p \quad (8)$$

(cf. (6)) allows to express the information by the signal phase at the end of the corresponding modulation interval. With the address vector

$$\boldsymbol{w}[i]\triangleq[\psi[i],\ldots,\psi[i-L]] \quad (9)$$

a modified signal table can be used. That is, the operation (8) is incorporated into the signal table definition and now, the signal elements are denoted by $\rho(\boldsymbol{w}[i],t)$, the transmitted signal by $s(\boldsymbol{\psi},t)$. Since the information is represented in the absolute phase, this structure is referred to as CPM with *phase–state mapping* [2] and illustrated in Fig. 1. Phase–state mapping can also be generated simply by the application of a discrete–time differentiator (Eq. (8)) to the input symbols of the CPM modulator with frequency mapping.

Of course, by applying such a differentiation the phase ambiguities due to the rotational invariance of CPM become unresolvable. Therefore, it should never be applied when using a coherent receiver with an explicit carrier phase synchronization unit, because a phase slip would cause a complete loss until a training sequence (e.g. frame synchronization word) appears. The situation is quite different for a noncoherent receiver combined with a convolutional encoder. Here,

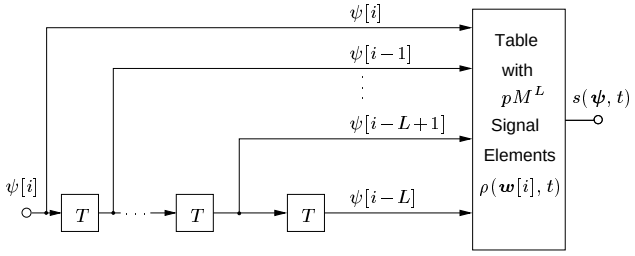


Figure 1: Decomposition of CPM with phase–state mapping.

phase ambiguities are resolvable due to a noncoherently non–catastrophic encoder [9, 10]. As phase estimation is part of the noncoherent decoding process, actual phase slips do not exist. They simply correspond to detours in the trellis decoding algorithm. Our investigations also showed that most of the known codes optimized for coherent transmission are rotationally variant, i.e., noncoherently non–catastrophic [10].

Phase–state mapping is perfectly matched to coded CPM using convolutional codes. For the sake of simplicity, we restrict ourselves to nonrecursive convolutional encoders with obvious minimum encoder structure. Due to the feedback–free shift register structure of the CPM encoder (Fig. 1), a fusion of the convolutional and the CPM encoder is possible, offering high power efficiency at a comparatively low receiver complexity.

The overall transmitter with $M'$–ary input data $u[l]$ of the convolutional encoder is illustrated in Fig. 2. In case of need, the information symbols $\psi[i]$ are generated from the coder output through some mapping.

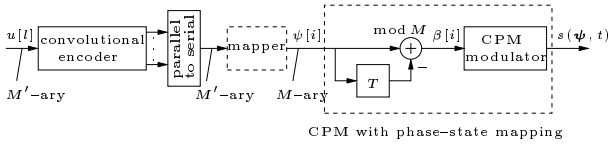


Figure 2: Transmitter structure for coded CPM with phase–state mapping. $M = p$.

## 2.3 Channel

We consider transmission over the additive white Gaussian noise (AWGN) channel with a signal phase unknown to the receiver. The received signal $r(t)$ may then be written as

$$r(t) = \mathrm{e}^{\mathrm{j}\phi(t)} \cdot s(\boldsymbol{\psi}, t) + n(t) \;, \tag{10}$$

where the unknown phase $\phi(t)$ is slowly time–varying and $n(t)$ denotes complex–valued AWGN with two–sided power spectral density $N_0$ in the ECB domain (corresponding to a physical channel noise with one–sided power spectral density $N_0$, as usual).

# 3 Noncoherent Receiver Structure

For the optimum receiver, a bank of $D \leq 2 \cdot M^L$ matched filters is required to deliver sufficient statistics for $r(t)$ [1]. In addition, detection has to be done by maximum–likelihood sequence estimation (MLSE) based on a super–trellis, which takes into account error correction coding, the trellis structure inherent to CPM, and the dependence among received samples due to the (slowly varying) unknown channel phase (see Section 3.2). If both filtering and sequence estimation are optimally solved, a very high computational complexity results. Thus, suboptimum receiver structures and signal processing requiring a low complexity are desired, whereas performance degradation should remain as small as possible. In contrast to previous approaches, e.g. [7], we treat these two problems separately.

## 3.1 Multi–Dimensional Matched Filter Front–End for CPM

Clearly, for a low receiver complexity a set of $D$ basis functions which represent the signal space spanned by $\rho(\boldsymbol{w}[i], t)$ as completely as possible for a given (small) value of $D$ has to be found. For this purpose, we adopt the reduction methods proposed by Huber and Liu [5] leading to a compact receiver front–end with very simple filter realizations. In [5] it is shown that the signal elements of almost all CPM schemes relevant in practice can be sufficiently represented by only $D = 2$ or $D = 3$ complex exponential functions of duration $T$. More specifically, the signal elements $\rho(\boldsymbol{w}[i], t)$ in the ECB domain are approximated by

$$\rho(\boldsymbol{w}[i], t) \approx \sum_{d=1}^{D} \rho_d(\boldsymbol{w}[i]) \mathrm{e}^{\mathrm{j}2\pi f_d t} \tag{11}$$

with[1]

$$f_d = \frac{\Delta f}{2}(2d - 1 - D) + h\frac{M-1}{2T} \tag{12}$$

and $1 \leq d \leq D$. Here, $\rho_d(\boldsymbol{w}[i])$ are the coordinates of $\rho(\boldsymbol{w}[i], t)$ with respect to the chosen basis of the CPM signal space, and $\Delta f$ denotes the frequency spacing parameter. The rational behind (11) is that time–limited functions can be well represented by samples in the frequency domain and using $\sin(\pi fT)/(\pi fT)$ functions for interpolation. Apparently, the frequency spacing parameter $\Delta f$ has to be optimized for maximum utilizable free Euclidean distance, for details we refer to [5]. The vector $\boldsymbol{\rho}(\boldsymbol{w}[i]) \stackrel{\triangle}{=} [\rho_1(\boldsymbol{w}[i]), \ldots, \rho_D(\boldsymbol{w}[i])]$ of coordinates is

[1] Note that due to the chosen ECB transformation frequency, $f_d$ differs by $\left(h\frac{M-1}{2T}\right)$ from that in [5].

obtained from

$$\boldsymbol{\rho}(\boldsymbol{w}[i]) = [\varrho_1(\boldsymbol{w}[i]), \ldots, \varrho_D(\boldsymbol{w}[i])] \cdot \boldsymbol{C}^{-1} , \quad (13)$$

where $\varrho_d(\boldsymbol{w}[i])$ are the *spectral samples* at frequency $f_d$

$$\varrho_d(\boldsymbol{w}[i]) = \int_0^T \rho(\boldsymbol{w}[i], t) \mathrm{e}^{\mathrm{j}2\pi f_d t} \, \mathrm{d}t \quad (14)$$

and $\boldsymbol{C}$ is the covariance matrix of the $D$ exponential basis functions.

The $D$ samples of the received signal at the $i^{\text{th}}$ modulation interval are arranged in the vector $\boldsymbol{r}[i] \triangleq [r_1[i], \ldots, r_D[i]]$ with

$$r_d[i] = \int_0^T r(t + iT) \mathrm{e}^{-\mathrm{j}2\pi f_d t} \, \mathrm{d}t , \quad 1 \le d \le D . \quad (15)$$

The receiver structure under consideration is also depicted in Fig. 3. We note that the used receiver front–end allows direct application of subsequent noncoherent detection methods used for linear modulation schemes, e.g. [9, 4, 11], i.e., a whitening filter necessary for the scheme in [7] is not required (see Section 3.2).

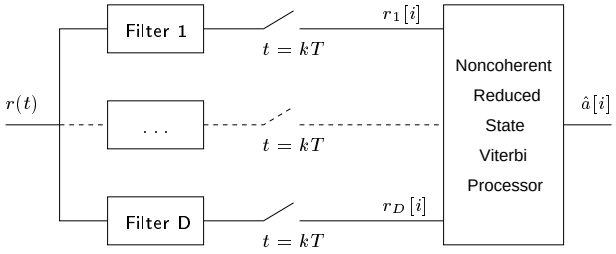


Figure 3: Frequency–sampling receiver and NSE.

## 3.2 Noncoherent Sequence Estimation for CPM

Now, optimum noncoherent sequence estimation (NSE) and suboptimum NSE with windowing of the observations are briefly described. Specifically, we introduce the concepts of a finite rectangular and an infinite, but exponentially decaying observation window. For derivation of the NSE metric for CPM we assume the unknown channel phase to be constant, i.e., $\phi(t) = \phi$. Later on, this restriction is relieved, and in the simulations presented in Section 4, the influence of a time–varying phase on the receiver performance is also investigated.

For a constant envelope signal and the AWGN channel with unknown phase the optimum NSE metric for a block of $N_T$ transmitted symbols $\psi[i]$, $0 \le i \le N_T - 1$, reads[2] [12, 4]

$$\Lambda[N_T - 1] = \mathrm{Re}\left\{ \sum_{i=1}^{N_T - 1} \boldsymbol{r}[i] \cdot \boldsymbol{\rho}^H(\tilde{\boldsymbol{w}}[i]) \cdot \left( \sum_{m=0}^{i-1} \boldsymbol{r}[m] \cdot \boldsymbol{\rho}^H(\tilde{\boldsymbol{w}}[m]) \right)^* \right\} , \quad (16)$$

where $\tilde{\boldsymbol{w}}[i]$ is constructed from $\tilde{\psi}[i]$ (9), which correspond via encoding to $M'$–ary hypothetical trial data symbols $\tilde{u}[l]$. From (16) the *incremental* metric $\lambda[i] \triangleq \Lambda[i+1] - \Lambda[i]$ at time $i$, $0 \le i \le N_T - 2$, follows as

$$\lambda[i] = \Re\left\{ \boldsymbol{r}[i] \cdot \boldsymbol{\rho}^H(\tilde{\boldsymbol{w}}[i]) \cdot \tilde{q}_{\text{ref}}^*[i-1] \right\} \quad (17)$$

with the definition $\tilde{q}_{\text{ref}}[i-1] \triangleq \sum_{m=0}^{i-1} \boldsymbol{r}[m] \cdot \boldsymbol{\rho}^H(\tilde{\boldsymbol{w}}[m])$. $\tilde{q}_{\text{ref}}[i-1]$ can be considered as *phase reference symbol*. In its present form, $\tilde{q}_{\text{ref}}[i-1]$ corresponds to an unlimited phase memory, which grows with time $i$. Hence, a tree search has to be employed for maximization of $\Lambda[N_T - 1]$. Moreover, the channel phase is required to be constant during the whole transmission time, which is usually not true in practice, of course.

To overcome these drawbacks, limitation of the phase memory has been proposed. Specifically, rectangular windowing [4] with window size $N \ge 2$, where $\tilde{q}_{\text{ref}}[i-1]$ is approximated by

$$\tilde{q}_{\text{ref}}[i-1] \triangleq \frac{1}{N-1} \cdot \sum_{m=1}^{N-1} \boldsymbol{r}[i-m] \cdot \boldsymbol{\rho}^H(\tilde{\boldsymbol{w}}[i-m]) \quad (18)$$

or exponential windowing [11] with forgetting factor $\alpha$, $0 \le \alpha < 1$, where the modified reference symbol is generated *recursively* from

$$\tilde{q}_{\text{ref}}[i-1] \triangleq \alpha \cdot \tilde{q}_{\text{ref}}[i-2] + (1-\alpha) \cdot \boldsymbol{r}[i-1] \cdot \boldsymbol{\rho}^H(\tilde{\boldsymbol{w}}[i-1]) \quad (19)$$

are promising approaches. Apparently, for the special cases $N = 2$ ($N \to \infty$) and $\alpha = 0$ ($\alpha \to 1$) (18) and (19) are identical.

In terms of computational complexity, exponential windowing compares favorably with rectangular windowing [11, 10]. For the former technique less arithmetic operations are necessary, and moreover, complexity is independent of $\alpha$. For rectangular windowing, however, complexity increases with $N$.

Clearly, now NSE can be performed by a full–state Viterbi algorithm in a super trellis taking into account the memory of convolutional coding, of CPM, and of the phase reference. In order to limit complexity of noncoherent CPM decoding, we employ per–survivor processing [13] and define a trellis diagram with $(M')^K$ states $S'[l] \triangleq (\tilde{u}[l-1], \ldots, \tilde{u}[l-K])$, $K \ge 0$. Here, the value of $K$ determines the exchange between performance and complexity. For $0 \le m \le K$, the hypothetical symbols $\tilde{u}[l-m]$ are defined by the transition from state $S'[l]$ to $S'[l+1]$. For $m > K$, the symbols $\tilde{u}[l-m]$ are taken from the surviving path terminating in state $S'[l]$. In case of

[2] Re{} denotes the real part of a complex number.

exponential windowing, each path in the trellis has its private reference symbol $\tilde{q}_{\mathrm{ref}}[i-1]$, which is updated according to (19) using the previous reference symbol $\tilde{q}_{\mathrm{ref}}[i-2]$ of the same path. At the end of each trellis branch only the reference symbol associated with the surviving path is stored and used for calculation of the first reference symbol of the next branch.

# 4 Simulation Results

To demonstrate the performance of the proposed noncoherent coded CPM transmission scheme, simulations of the bit–error rate (BER) versus $E_b/N_0$ ($E_b$: received signal energy per information bit) have been performed first. For these simulations, the channel phase $\phi(t)$ is kept constant. Eventually, we will consider channels with time–variant phase $\phi(t)$, too.

As an important example of coded binary CPM with $h = 1/2$, we consider Gaussian minimum–shift keying (GMSK) with 3 dB bandwidth–bit–duration product $BT = 0.3$. For coding, the binary rate $1/2$ convolution code with 16 states (generator polynomials $\boldsymbol{g}_1 = (2,3)$, $\boldsymbol{g}_2 = (3,5)$ (base–8 representation))) from [9, Table I] is taken. At the receiver, a front–end with $D = 2$ filters is applied. NSE and coherent MLSE are performed on a trellis with 32 states, i.e. NSE based on per–survivor processing is employed. In case of coherent CPM, further expansion of states is not rewarding [10]. The numerical results for noncoherent reception with rectangular and exponential windowing are presented in Figs. 4a) and b), respectively. Although states are reduced to a great extent, by increasing the observation interval of NSE, the performance of coherent reception with perfect phase synchronization is approached. This is true for both windowing techniques. More specifically, it is always possible to find pairs of ($N$, $\alpha$) yielding similar performance [10]. Hence, the complexity advantages of exponential windowing can be fully exploited.

It is of high interest to discuss coded noncoherent *multilevel* CPM, because in the coherent case the best trade–off between power and bandwidth efficiency is found for 4 and 8–ary CPM. For this reason, we regard 2RC 4–ary CPM with $h = 1/4$, i.e., the frequency pulse $g(t) = \mathrm{d}q(t)/\mathrm{d}t$ is a raised cosine pulse with duration $L = 2$. A 4–ary rate $1/2$ code with 16 states is chosen (generator polynomials $\boldsymbol{g}_1 = (1,3,3)$ and $\boldsymbol{g}_2 = (2,3,1)$ (base–4 representation)), which is also taken from [9, Table I]. Again, $D = 2$ is applied. For coherent reception of CPM, the joint code and modulator trellis has 64 states. As for GMSK, NSE with per–survivor processing is performed on the same trellis. The obtained results are depicted in Figs. 5a) and b) for rectangular and exponential windowing, respectively. Remarkably, without increasing complexity in terms of decoder states, the proposed noncoherent CPM approaches the power–efficiency of coherent

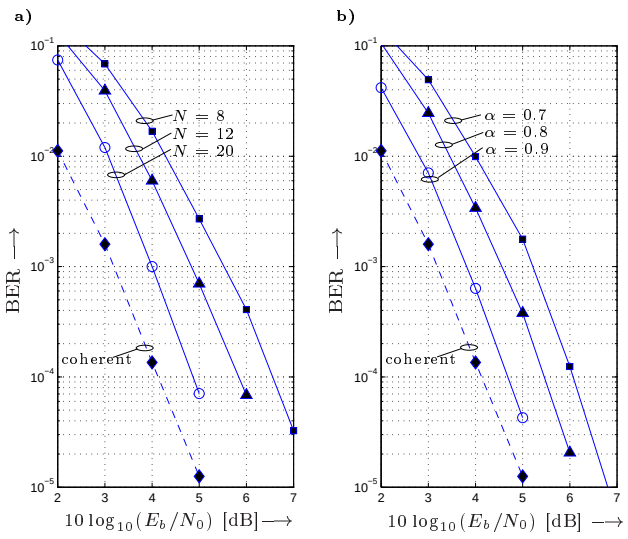


Figure 4: BER vs. $E_b/N_0$ for the proposed CPM system. GMSK with $BT = 0.3$ and a 16–state binary rate $1/2$ code. $\phi(t) =$ constant. NSE and coherent MLSE with 32 states, respectively. a) rectangular windowing. b) exponential windowing.

reception. Again, recursive calculation of the reference symbol with low complexity (19) performs very well.

In the above two examples of noncoherent CPM, we increased the number of trellis states of the underlying code by a factor of $M'$ (i.e. the state representation is extended by only a single hypothetical information symbol $\tilde{u}[l]$). The results show that this way of modeling the memory of both CPM and channel phase, provides a favorable trade–off between complexity and performance. This has been verified for various modulation parameters [10].

Finally, the robustness of the proposed scheme to phase jitter is assessed. The phase $\phi(t)$ has been modeled as a Wiener process, i.e., the sequence of phase changes is a white Gaussian noise process with variance $\sigma_\Delta^2$ over $T$. This model is frequently used, e.g. [4, 8]. 2RC 4–ary CPM with the same parameters as in Fig. 5 has been simulated. Fig. 6 shows the measured BER's as a function of $\sigma_\Delta$ for $E_b/N_0 = 5$ dB. Clearly, there is an exchange between the achievable power efficiency for $\sigma_\Delta = 0$ and the robustness against phase noise. As $\alpha$ ($N$) increases, the robustness against phase variations deteriorates, while the power efficiency for $\sigma_\Delta \to 0$ improves. Consequently, in practice $\alpha$ ($N$) has to be adapted to the current situation. Since $\alpha$ is a real number, but $N$ is integer, the lower–complex metric facilitates optimization. In particular, for given $E_b/N_0$ and phase noise variance $\sigma_\Delta^2$ the minimum achievable BER can always be attained exactly.

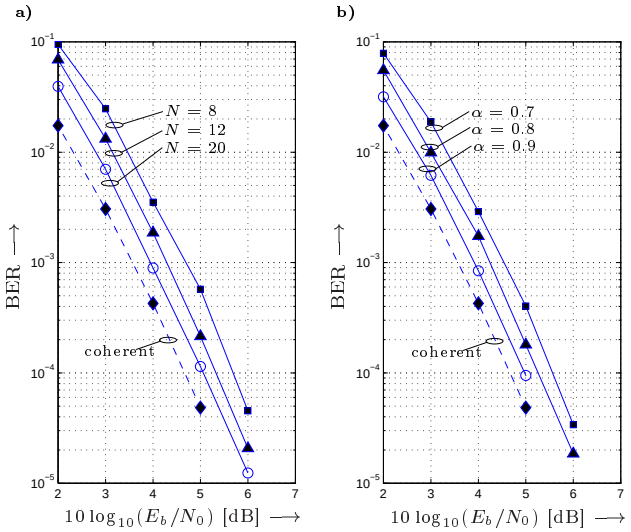


Figure 5: BER vs. $E_b/N_0$ for the proposed CPM system. 2RC 4–ary CPM with $h = 1/4$ and a 16–state 4–ary rate 1/2 code. $\phi(t) =$ constant. NSE and coherent MLSE with 64 states, respectively. a) rectangular windowing. b) exponential windowing.

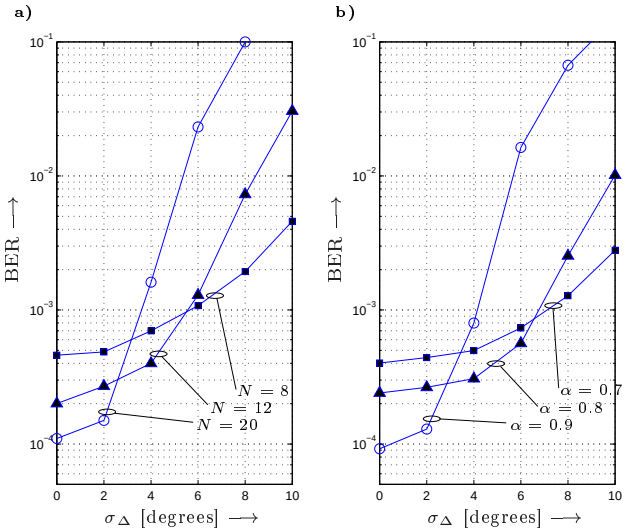


Figure 6: BER vs. the jitter standard deviation $\sigma_\Delta$ per modulation interval for the proposed CPM system. 2RC 4–ary CPM with $h = 1/4$. Parameters as in Fig. 5. a) rectangular windowing. b) exponential windowing.

# 5 Conclusions

Coded noncoherent CPM transmission over the AWGN channel with unknown phase is discussed. We employ the decomposition of CPM into a continuous–phase encoder and a memoryless mapper and perform differentiation of modulator input data to combine efficiently CPM with rotationally variant convolutional coding. The decomposition of CPM facilitates our receiver design within two stages. For low–complex receiver input filtering an advantageous receiver front–end is applied. To enable noncoherent reception, appropriate metrics used for Viterbi decoding are specified. For a slowly time–varying channel phase the power efficiency of coherent CPM (assuming perfect knowledge of the channel phase) is approached. Remarkably, this is achieved *without* increasing the number of trellis states in comparison to coherent MLSE. Moreover, recursive branch–metric calculation is successfully applied to CPM and thus, complexity is further reduced. To summarize, the proposed CPM scheme is attractive for power and bandwidth–efficient noncoherent transmission with very moderate transmitter and receiver complexity.

# References


[1] J. Anderson, T. Aulin, and C.-E. Sundberg, *Digital Phase Modulation*. New York: Plenum Press, 1986.

[2] J. Huber and W. Liu, "Convolutional Codes for CPM Using the Memory of the Modulation Process," in *Proc. IEEE Global Telecom. Conf.*, (Tokyo), pp. 43.1.1–43.1.5, 1987.

[3] B. Rimoldi, "A Decomposition Approach to CPM," *IEEE Trans. Inf. Theory*, vol. 34, pp. 260–270, Mar. 1988.

[4] G. Colavolpe and R. Raheli, "Noncoherent Sequence Detection," *IEEE Trans. Com.*, vol. 47, pp. 1376–1385, Sept. 1999.

[5] J. Huber and W. Liu, "An Alternative Approach to Reduced–Complexity CPM–Receivers," *IEEE J. Select. Areas Commun.*, vol. 7, pp. 1437–1449, Dec. 1989.

[6] R. Schober, L. Lampe, and G. Enzner, "Noncoherent Sequence Estimation: A Comparison," in *Proc. IEEE Int. Conf. Telecom. (ICT)*, (Bucharest), June 2001.

[7] G. Colavolpe and R. Raheli, "Noncoherent Sequence Detection of Continuous Phase Modulations," *IEEE Trans. Com.*, vol. 47, pp. 1303–1307, Sept. 1999.

[8] D. Raphaeli and D. Divsalar, "Multiple–Symbol Noncoherent Decoding of Uncoded and Convolutionally Coded Continuous Phase Modulation," *J. Commun. and Networks*, vol. 4, pp. 238–248, Dec. 1999.

[9] D. Raphaeli, "Noncoherent Coded Modulation," *IEEE Trans. Com.*, vol. 44, pp. 172–183, Feb. 1996.

[10] G. Enzner, "Noncoherent Sequence Estimation for Coded M(D)PSK and CPM Transmission," *Master Thesis, University of Erlangen–Nürnberg*, 2000.

[11] R. Schober and W. Gerstacker, "Metric for Noncoherent Sequence Estimation," *Electr. Letters*, vol. 35, pp. 2178–2179, Dec. 1999.

[12] J. G. Proakis, *Digital Communications*. New York: McGraw–Hill, third ed., 1995.

[13] R. Raheli, A. Polydoros, and C.-K. Tzou, "Per–Survivor Processing: A General Approach to MLSE in Uncertain Environments," *IEEE Trans. Com.*, vol. 43, pp. 354–364, Feb./Apr. 1995.